RSC Advances

ROYAL SOCIETY OF CHEMISTRY

www.rsc.org/advances

Correlation of Mo dopant and Photocatalytic Properties for Mo incorporated TiO_2: An EXAFS and Photocatalytic Study

Jerina Majeed[a], C. Nayak[b], S. N. Jha[b], Kaustava Bhattacharyya[a]*, D. Bhattacharyya[b]*, A. K Tripathi[a]

[a] - Chemistry Division, [b] Atomic & Molecular Physics Division,

Bhabha Atomic Research Centre, Mumbai – 400085, INDIA

Corresponding Author:

Dr. Kaustava Bhattacharyya

Chemistry Division

Bhabha Atomic Research Centre

Mumbai-400085, India.

Office Phone:+0091- 22- 25590271

Fax: 0091-22-2550 5151

0091-22-2551 9613

Email: *kaustava@barc.gov.in*

Abstract:

The present study envisages the quantitative estimation and understanding of the nature of phases present in the Mo-incorporated titania through extensive EXAFS measurements (at Mo K-edge and Ti K-edge) and to decipher their role in photodegradation of Methylene Blue (MB) dye under UV and visible irradiation. EXAFS results revealed presence of both MoO_3 nano heterophase phase and substitutional Mo dopants in TiO_2 lattice, the extent of later was reduced with the increasing Mo content of the sample. Presence of MoO_3 in the Mo-incorporated titania was also revealed by the FT-IR and TEM studies. Photocatalytic studies have shown considerable adsorption of the cationic MB-dye perhaps due to the electronic interaction between the dye and catalytic surface. Under visible irradiation, the photocatalytic activity followed the trend: Mo-5 > Mo-2 > Mo-1 > Mo-10 >> TiO_2, while the trend for photodegradation of MB dye under UV irradiation was as follows: Mo-5 > Mo-2 > Mo-1 > TiO_2 > Mo-10. These results have been explained in the light of the structural properties of the Mo-TiO_2 system obtained from EXAFS measurements. It has been observed that relative ratio of substitutional Mo-dopant to MoO_3 phase in this tri-phasic photocatalysts plays a crucial role in augmenting their oxidative photocatalytic property.

Keywords: *Mo-TiO_2 –system; EXAFS; photocatalytic degradation of MB-dye; structure – activity correlation.*

1. Introduction:

TiO_2 is one of the most efficient photocatalysts, among the semiconductors due to its high catalytic activity, long lifetime of photogenerated carriers [1], high chemical stability, and nontoxicity [2-4]. However, the photo efficiency of TiO_2 is limited by its intrinsic wide bandgap which allows only UV region of the spectrum to be absorbed. It uses only 3-5% of the solar spectrum as its absorption decreases drastically in visible region. Recently, a lot of attempts have been made to reduce the bandgap of TiO_2 by doping transition metals into TiO_2 [5-8]. The reduced bandgap will result in an increase in the absorption of TiO_2 in the visible region which in turn will ensure an enhanced photo activity under solar light irradiation [9]. If a transition metal such as Mo is doped into the TiO_2 lattice, these dopant ions can either segregate on TiO_2 nanostructure surface or they can be incorporated into the lattice. The dopants can be substitutional, interstitial or both when incorporated. It is mostly the substitutional dopant ions that contribute to the change of electronic structure and light absorption efficiency of the host. The substitutional dopant ions can induce an electronic coupling effect with the host atom and bring possible electron states within the band gap of the semiconductors [10]. The dopant related localized states on either above the valence band or below the conduction band are favorable to the band gap change, which in turn affects the photon absorption [11].

Dopants with different locations in the host matrix have different impact on the photo-catalytic properties of TiO_2. For example, in our earlier study [12] on the photo-degradation of Rh-B dye under UV irradiation with Mo doped TiO_2 as a photocatalyst, it has been found that, catalytic activity of Mo-TiO_2 samples with different Mo concentration is mainly guided by TiO_2 concentration in the material. However, in the present communication, where the activity of the

same Mo-TiO_2 photocatalysts has been tested on another important dye material i.e., Methylene Blue (MB), we have found that the trend of variation of photocatalytic activity with Mo doping concentration is different, which warrants further microscopic structural analysis of this photocatalyst. Almost 15% of the entire dyes manufactured in the textile industry worldwide are released as the textile effluents. The dyes and the modified chemical products of these dyes released in the ecosystem is basically a tremendous source of pollution, eutrophication and perturbations in the aquatic life, as well instigate several diseases in the human beings. They should therefore be degraded/ mineralized completely at the fastest rate. The Methylene Blue dye is taken as a model dye for the dyes used in the leather and other textile industries.

The location and the local bonding configuration of the dopants in TiO_2 matrix is found to be very important for predicting its photo-catalytic performance in different dye systems. In our earlier work [12], for Mo doped TiO_2 samples, we had proposed the presence of both the nano-heterostructure of MoO_3 with that of TiO_2 anatase structure along with certain percentage of Mo being doped (substituted) in the anatase TiO_2 lattice. However, that was an indirect prediction based on the results obtained from the XRD, TEM and other spectroscopic techniques like Raman and XPS [12]. In the present communication we have employed a more direct technique viz., Extended X-ray absorption fine structure (EXAFS) to probe the local structure of the dopants in the host matrix microscopically and to understand its influence on photocatalytic properties of Mo/TiO_2 photocatalyst.

A few EXAFS studies on Mo doped TiO_2 photo-catalytic system has already been reported in the literature, though the results are found to be varied widely. For example, while Feng et. al.[13] have found by EXAFS measurements on their photocatalytic samples prepared by co-deposition method that Mo was substituting Ti in TiO_2 lattice as Mo^{+6}, EXAFS

measurements by Scheider et. al.[14] on their samples synthesized by Flame Spray Synthesis (FSS) process revealed substitution of Mo in TiO_2 lattice with high cationic vacancies around Mo cations. Kubacka et. al. [15] on the other hand have found significant MoO_x clustering on the surface of their microemulsion-prepared Mo doped anatase TiO_2 along with Mo^{6+} substitution of Ti^{4+} ions by EXAFS, XPS and Raman measurements. This shows the local structure of these samples around Mo cation is strongly dependent on the preparation method.

In the present study, Mo K-edge and Ti K-edge EXAFS measurements have been carried out on Mo doped TiO_2 samples prepared in a modified sol-gel process with different doping concentrations of Mo and the data has been analyzed to study the structural changes at different doping levels. EXAFS measurements have also been supported by FT-IR and TEM measurements. Most of the earlier studies on doped catalytic systems, deal with qualitative dependence of the photocatalytic activity of the catalyst on the concentration of the dopants. In this work we have tried to correlate the photocatalytic activity with quantitative information of different phases present in the doped system, which to the best of our knowledge has been discussed very rarely in the literature.

2. Experimental:

a. Synthesis

A simple method was employed for the preparation of the nanotitania and Mo-doped (1-10 atom %) titania [12]. In this modified sol-gel process, the required stoichiometric amount of molybdic acid (Aldrich, 97%) was initially dissolved in nano pure water [conductivity18.2 megohm-cm ionic purity and 1–5 ppb total organic carbon content] at room temperature at a neutral pH. The molybdic acid solution was maintained at 0 °C by external application of ice-salt

mixture. To the molybdic acid solution, Ti (IV) iso-propoxide solution in iso-propanol (IPA) was added drop wise in a controlled manner. This gel was stirred further to ensure incorporation of molybdenum precursor in the titanium gel phase and dried. The resulting solid mass was crushed and calcined at 500 °C for 4 h. This method is discussed in details elsewhere [12]. Henceforth, the undoped TiO_2 (anatase) and the Mo-TiO_2, MoO_3, would be denoted as Mo-0, Mo-1, Mo-2, Mo-5, Mo-10, and Mo-100, where the suffix denotes the atom% of Mo in the sample.

b. Characterization

The EXAFS measurements on the Mo doped TiO_2 samples were carried out in the BM-29 scanning EXAFS beamline in the European Synchrotron Radiation Facility (ESRF), Grenoble, France, operating at 6 GeV in 16-bunch filling mode with electron beam currents ~100 mA. Considering the small content of Mo within the TiO_2 matrix, the EXAFS spectra were taken in the fluorescence mode with a 13 element fluorescence detector and choosing only the K_β emission lines so the signal does not get perturbed by the fluorescence yield from Ti matrix. EXAFS measurements of the samples at Ti K edge were carried out at the Scanning EXAFS Beamline (BL-9) at the INDUS-2 Synchrotron Source (2.5 GeV, 100 mA) at the Raja Ramanna Centre for Advanced Technology (RRCAT), Indore, India [16]. The EXAFS spectra of the samples at Ti K edge were recorded in the energy range 4930-5300 eV in the transmission mode.

The FT-IR spectra of the solid samples in the mid IR region (4000–400 cm^{-1}) were recorded in KBr using a FTIR spectrophotometer (model- JASCO 610) equipped with a DTGS detector having a resolution of 4 cm^{-1}. For this purpose about 200 mg of dry KBr was mixed with 5 mg of the sample, ground and pressed into a transparent, thin pellets at 5 tons/cm^2. Transmission electron microscope (TEM) data were obtained using a 120 keV and a 200 kV FEI

Technai machine equipped with a LaB_6 filament. TEM samples were prepared by placing a drop of the ultrasonically dispersed powder (in alcohol) on a carbon-coated copper grid and drying in air. Energy dispersive X-ray (EDS) spectroscopy was used to determine the elemental composition of the samples.

c. **Photocatalytic Studies**

Molybdenum doped TiO_2 samples so obtained were evaluated as photocatalysts for the degradation of Methylene Blue (MB) dye in the presence of UV light. A 100 ml batch cylindrical pyrex glass reactor was employed (basically a glass beaker of 100 ml) and the irradiation source was medium pressure Hg lamp (SAIC) located inside a quartz tube, situated horizontally in the reactor with 170 mW/cm^2 flux. A broad range source having emission in the range from 350 to 700 nm with maxima at ~ 430 nm and with a flux of 234 mW/cm^2 was used for irradiation in the visible region. For each set of experiments, the reaction mixture consisted of 50 mg of catalyst powder suspended in 100 ml of the dye solution (~10^{-5} M concentration of the Dye). The suspensions were magnetically stirred for 30 min in the dark to establish adsorption/desorption equilibrium. The dye-catalyst suspensions were irradiated under UV light and small aliquots were withdrawn at regular intervals of time (keeping the volume of reaction mixture almost constant) and UV-visible spectra were recorded. A blank consisting of only aqueous MB solution (dye, without the catalyst), was also subjected to same procedure to cancel the effect of self-degradation of the dye. The extent of reaction was monitored by measuring the decrease in absorbance values using UV-Visible-NIR spectrometer (model-JASCO V-670).

3. Results and Discussions:

a. EXAFS study

Figure S.I.1 shows the experimental EXAFS ($\mu(E)$ versus E) spectra of the Mo doped TiO_2 samples at Mo K edge. Each energy spectrum is reduced to a plot in wavenumber scale (k) following the standard procedure [17] and the $\chi(k)k^2$ versus k plots for the Mo doped TiO_2 samples have been shown in Fig.1. It can be observed from Fig. 1 that the plots of 10% Mo doped sample is significantly different from that of other samples. Finally the wavenumber plots are Fourier transformed to generate the radial distribution functions, the k range used for Fourier Transform being 3-12 $Å^{-1}$. It should be mentioned here that a set of EXAFS data analysis program available within the IFEFFIT software package [18] have been used for reduction and fitting of the experimental EXAFS data with theoretically generated spectra. The bond distances and disorder (Debye-Waller) factors (σ^2), which give the mean-square fluctuations in the distances, have been used as fitting parameters. The quality of fitting has been determined by minimizing the *R-factor* defined as the fractional misfit between experimental data and theoretical fit:

$$R\ factor = \frac{\sum_{i=min}^{max}[Re(\chi_d(r_i) - \chi_t(r_i))^2 + \mathrm{Im}(\chi_d(r_i) - \chi_t(r_i))^2]}{\sum_{i=min}^{max}[Re(\chi_d(r_i))^2 + \mathrm{Im}(\chi_d(r_i))^2]} \qquad (1)$$

Figure 2 shows the theoretical EXAFS radial distribution functions ($\chi(r)$ versus r) for MoO_3 structure and Mo doped TiO_2 structure generated by assuming σ^2 to be 0.003 and Fig. 3 shows the experimental $\chi(r)$ versus r plots of the Mo doped TiO_2 samples. Comparing the experimental and theoretical plots, it can be seen from the first two peaks that MoO_3 phase is dominantly present in these samples. However, the peak denoted by an arrow in Fig. 3 is representative of Mo in TiO_2 structure which leads to the conclusion that both the phases viz., MoO_3 and Mo substituted in TiO_2 lattice are present in these samples. Subsequently, the experimental $\chi(r)$ versus r plots of these samples have been fitted from 1-4 Å assuming both

MoO_3 and Mo in TiO_2 lattice phases. It should be mentioned here that the fitting attempted assuming single phase i.e. MoO_3 structure or Mo in TiO_2 structure does not give a good fit with physically acceptable parameter values (Fig. S.I.2, supplementary information) and the two-phase fitting considerably improves the fitting quality of the data. This strongly indicates the presence of both MoO_3 and Mo doped TiO_2 phases in the present samples, which is also corroborated by FT-IR and TEM studies discussed later in this section. It should also be noted that since there is no signature of extra Mo-Mo peak at a relatively lower R values in the experimental radial distribution function of the samples, the probability of Mo ions in the interstitial positions are ruled out and this option was not considered in the fitting of the FT-EXAFS spectra of the samples.

To get a quantitative idea about the two phases, a new fitting parameter x has been defined and all paths corresponding to MoO_3 structure has been weighted by x while the paths of Mo in TiO_2 structure have been weighted by (1-x). The structural parameters for MoO_3 and TiO_2 structure are obtained from the literature [19, 20]. The parameter x denotes the fraction of MoO_3 phase in the samples and (1-x) will give the fraction of Mo going into TiO_2 lattice. In the fitting process the data are first fitted with only MoO_3 structure and the fitting are later improved by adding the contribution of substituted Mo in TiO_2 lattice and the "x" parameter. Further the coordination numbers (CN) which determine the strength of the scattering have not been varied for the different paths during fitting to obtain reliable information for the x value and we have assumed that Mo replaces Ti in Mo^{4+} state. This has helped in keeping the number of variable parameters in fitting low so that reliable and physically meaningful results are obtained. The best fits obtained by the above mentioned procedure have been shown in Fig. 3 and the fitting results have been tabulated in Table 1. The errors in the last decimal place are given in brackets.

The *R factors* of these fits are less than 0.01 which assure good fit of the data. It can be seen from Table 1 that as Mo doping concentration in TiO_2 increases, the percentage of Mo cation going into the TiO_2 lattice decreases and for 10 at.% Mo doped sample about 93% of the Mo cations exist in MoO_3 phase and only 7% goes into the TiO_2lattice. Presence of a separate Mn_2O_3 oxide phase has been observed by us in Mn doped ZnO system also [21].

Figure S.I.3 shows the experimental EXAFS ($\mu(E)$ versus E) spectra of the Mo doped TiO_2 samples at Ti K edge. The experimental $\chi(r)$ versus r spectra have been fitted from 1-2 Å (only the first coordination shell) with a Ti-O shell at 1.94 Å(×6) and the best fit have been shown in Fig. 4, while the results of the above fit has been tabulated in Table 2. The fitting results do not show any significant change in the first oxygen shell surrounding Ti in the samples with increase in Mo concentration. From Table 1 and 2, it can be seen that the Mo-O bond lengths of the Mo in TiO_2 lattice phase are less than Ti-O bond lengths. This is due to the lower ionic radii of Mo cations as compared to the Ti cations. However, the Mo-Mo bond lengths of MoO_3 phase decreases with increase in doping concentration. The first Mo-O bond length remains unchanged however, the second and third oxygen shell bond lengths decrease with increase in doping concentration. Therefore, the average Mo-O bond length decreases for MoO_3 phase with increase in doping concentration.

b. FT-IR Spectroscopic Studies

Figure 5 shows the IR spectra of the bulk anatase, the Mo-TiO_2 samples (Mo-1, Mo-2, Mo-5 and Mo-10), and MoO_3. Orthorhombic MoO_3 belongs to theD_{2h}^{16}(Pbnm) space group [22]. Factor group analysis of the D_{2h}^{16} group yields 45 distinct vibrational modes. Of these 17 modes are IR active. The frequencies (in cm^{-1}) for the MoO_3 sample are as follows: 3750, 3137, 1506,

1412, 1360, 1287, 1117, 999, 884, 627 cm^{-1}. Amongst these the vibrations between 1500 and 600 cm^{-1} are the ones related to the Mo-O vibrations whereas the others mainly correlate to the adsorbed –OH or H_2O stretches over the MoO_3 surface or act as an water of crystallisation. The most prominent band at 627 cm^{-1} is due to the ν O-Mo antisymmetric bend [20], at 999 cm^{-1} is due to Mo=O asymmetric stretching modes of terminal (unshared) oxygen [23, 24] and those at 884 and 1117 cm^{-1} are due to Mo=O stretching vibrations [24]. Figure 5 (A-a) represents the IR spectrum of anatase titania, which has tetragonal unit cell and belongs to the space group D_{4h}^{19}(I41/amd) [25, 26]. According to the factor group analysis, there are 15 different vibrational modes, of which 4 are IR–active modes. For the bulk titania sample, the spectrum shows a broadband in the 400-900 cm^{-1} region with peaks at ~ 470, 590, and 645 cm^{-1}. These bands have been assigned to the bending vibrations of the Ti-O-Ti bond of anatase titania [27].

The Mo-TiO_2 samples present a very exciting account. The above discussion reveals that both the anatase TiO_2 and MoO_3 has the vibrational peak at ~ 600 cm^{-1}. If we take a closer look in the 1500 - 400 cm^{-1} region (Fig. 7-B) we find that right from the Mo-1 sample there exists peaks at 958 and 1117 cm^{-1} which are the mark of MoO_3 phase along with the anatase TiO_2 peaks. As we go from the Mo-1 to Mo-10 this peak at 958 cm^{-1} grows in intensity and in Mo-10 shifts to 995 cm^{-1}. The Mo-10 sample possess all the features of that of MoO_3 like bands at 1407, 1117, 995 and 854 cm^{-1} which are the prominent peaks for the Mo-O along with that of anatase TiO_2.

The above results obtained from FT-IR studies thus shows that the Mo-TiO_2 samples are nano-composites in nature which corroborate excellently with our previous results of Raman studies on the samples [12]. However from the Raman studies we were able to substantiate that the MoO_3 phase was present more on the surface for the samples of Mo-1, Mo-2 and Mo-5,

while in samples with higher Mo-concentration like Mo-10, the bulk component increases [12]. The FT-IR data usually represent the bulk information and therefore here we find that with the increment in the Mo concentration in the samples, the MoO_3 phase becomes more prominent which corroborates with the EXAFS data also presented above.

c. Transmission Electron Microscopy studies (TEM)

Figure 6 shows typical transmission electron micrographs of Mo-2 samples (a representative sample of the others) along with its respective selected area electron diffraction (SAED) pattern. The d-spacing as shown in Fig. S.I.4 show the co-existence of both the nano heterophases of MoO_3 and that of TiO_2. The micrographs suggest that the samples consist of nano particles in the range of 7-10 nm, which are mostly spheroidal in shape. A close examination of the SAED patterns presented in Fig. 6 C confirms the co-existence of both TiO_2 and the MoO_3 in the Mo-2 sample. The SAED pattern for Mo-2 and Mo-10 could be indexed in the following reflections as given in the Table A and B in the S.I. (Fig. S.I.5, supplementary information). The SAED pattern of Mo-2 matches with that of TiO_2 anatase and that of Mo-10 matches more closely to that of MoO_3. TEM result, thus reveal the presence of both Mo-doped TiO_2 and MoO_3 phases in the samples, in conformity with our IR and EXAFS results.

d. Photocatalytic studies for Methylene Blue (MB) dye degradation.

Adsorption profiles of the samples were obtained by equilibrating the samples with the dye solution in dark for 30 min followed by recording the UV-Vis spectra. First, the absorbance was recorded in the blank experiment at different time intervals for pure MB-dye excluding any photocatalyst whatsoever. This shows peak maximum at 663 nm along with shoulder at 611 nm.

However, no significant decrement was observed and therefore it could be inferred that negligible self-degradation of the dye is present here (Fig. S. I. 6, supplementary information). The adsorption of MB-dye on nano TiO_2 sample is shown in (S. I.9) which reflects very little change in the UV-Vis spectra of the dye. However, unlike the pure titania sample, for all the Mo-TiO_2 samples, within 30 min of equilibration of the dye and the catalyst, almost 90% adsorption of the dye on the catalyst surface is observed (S.I.10) resulting in significant change in UV-Vis spectra of the dye. This suggests to a strong electronic interaction between the MB-dye and the catalytic surface of Mo-TiO_2 samples where concentration of surface hydroxyl group is found to be higher than titania (Fig.5) possibly resulting in higher surface charge density. The strong sorption behavior of MB-dye on catalyst surface hints us that preferably surface charge of the photocatalyst is optimum for adsorption of the cationic MB dye. Perceivably therefore changes in the morphological and electronic transformations owing to structural changes created by doping or the formation of nano hetero-structures will have a direct impact on the photocatalytic efficiency of these materials.

The photocatalytic activity of these materials was studied under ambient conditions using a photo-irradiation UV source as described earlier in the experimental section. Differential decrement in intensity of adsorption peak maxima of MB (663 nm) along with time was monitored and post adsorption the photodegradation of dye was also studied (Fig. S.I. 8 and 9-supplementary information) [28].

In case of pure TiO_2 which is UV active, complete degradation of the dye occurred in about 60 min (Fig.7). New peaks were not observed during the course of the photo-irradiation and intensities of all the peaks are decreased gradually with time. Also, no shift in the peak positions during irradiation indicated complete degradation of the dye molecule. Considering $t_{1/2}$

(time required for 50% reduction in the dye concentration) as a measure of the photocatalytic activity performance the $t_{1/2}$ values were derived from Fig.7 for pure titania and all the Mo incorporated titania samples. These values for the Mo-1, Mo-2, Mo-5, Mo-10 and titania samples were found to be ~3.4, 3.1, 2.9, 16.1, 9.9 min, respectively, representing following trend in photocatalytic activity for dye degradation: Mo-5 > Mo-2 > Mo-1 > TiO_2 > Mo-10.

This apparently tends to suggest that the process of adsorption, which in its own turn will be governed by surface charge, plays a major role for MB dye degradation. If we compare Fig. S.I.8 and Fig S.I.9 it would be very clear that the process of adsorption is quite significant for the Mo-TiO_2 system as compared to that of the nano TiO_2 system itself. Surface charge becomes more negative according to the zeta potential values with increase in Mo content in TiO_2 for the Mo-TiO_2 system [12] and MB being a cationic dye will definitely be better adsorbed on the surface with increase in Mo-content. Though the MB dye is adsorbed and the process of adsorption plays a strong role we have found that in the photocatalytic process the adsorbed dye itself could be degraded (Fig. S.I.11) and the photocatalysts could definitely be recycled at least for 3 cycles.

Here we should stress upon the difference between the adsorption behavior of MB dye described here and that of Rh-B-dye which had been discussed in our earlier communication. Since both the dyes are cationic dyes, the difference in their behavior perhaps lies in the difference in their structural properties. The positive charge over the N+ will be much more dispersed owing to the stronger (+I effect) by O in the Rh-B and more over the extra Ph-COOH will make more resonating structures to lower the overall positive charge over the $>N^{+}(Me)_2$ group. However in MB–dye the (+I) is via a –S (thio in the adjacent hetero ring). Therefore the MB dye will behave as a stronger cationic dye, having a stronger electronic interaction with the

negatively charged catalyst surface and this is reflected in comparative adsorption behaviors of the two dyes. The same set of photocatalysts of Mo-TiO_2 does not have a strong dark reaction (i.e. adsorption phenomena mainly) for the Rh-B dye whilst for the MB-dye there is very strong adsorption of the dye in general on the photocatalytic surface.

The process of adsorption of the MB dye on the surface of the Mo-TiO_2 photocatalysts can be shown schematically as follows. Here Scheme-1 portrays the MB molecule and Scheme-2 shows the adsorption phenomenon. To explain the strong adsorption process of the MB dye on the catalytic surfaces we propose that the option III of the Scheme-2 is the most followed route for the adsorption process. Here we can definitely neglect the lower probable anion – anion interaction of the MB –dye on the surface [29]. However, going by this analogy, the Mo-10 should have been the best catalyst, though as can be seen from Fig.8 that it is not the one and is even worse than the pure TiO_2 sample.

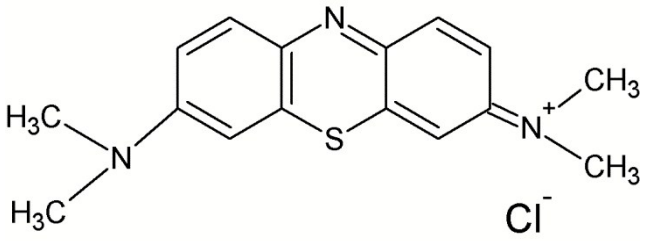

Methylene Blue Dye

Scheme-1

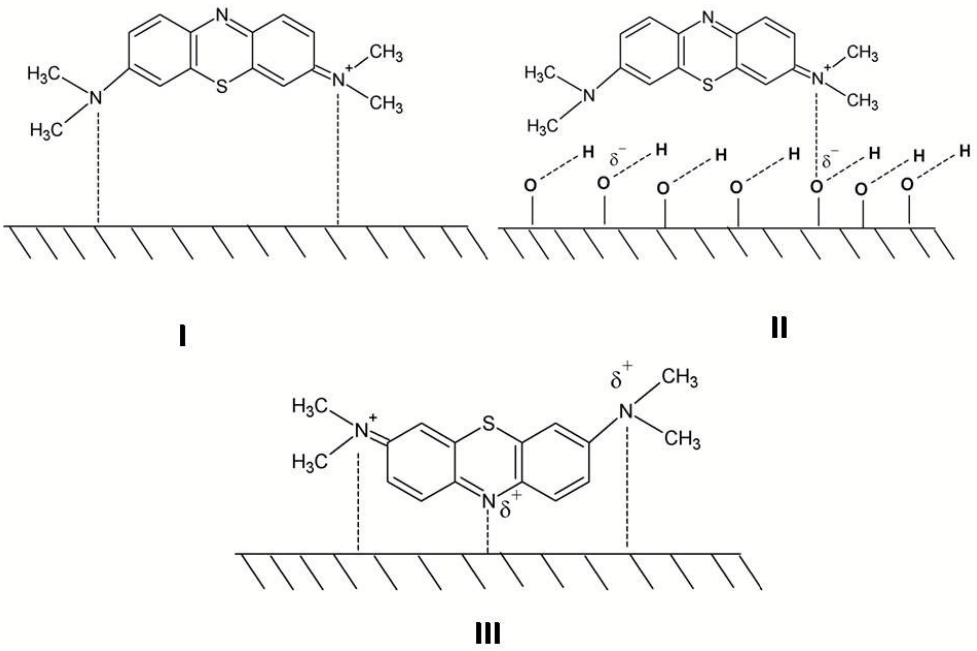

Scheme-2

From the characterization by EXAFS, FT-IR and TEM studies presented above and the Raman data presented in our earlier communication[12] we have conclusively shown that the samples discussed here consist of three phases viz., a MoO_3 nano-heterophases, a Mo substituted in TiO_2 anatase lattice phase and pure TiO_2 anatase phase. The nano-heterophases of MoO_3 will definitely change the red-ox potential of the Mo-TiO_2 photocatalysts as compared to that of only TiO_2. Similarly, the doped Mo will also shift the red-ox potential of the TiO_2 lattice in a positive direction to enhance its photocatalytic ability along with its role in shifting the band gap of the TiO_2 as a function of Mo content (however the nano-heterophases will also result to it). Therefore it is quite conclusive that the presence of Mo in the TiO_2 lattice augments its photocatalytic behavior but that happens with an optimum presence of Mo in the lattice. Now the question that needs to be answered at this juncture is whether nano-heterophases of MoO_3 or Mo atoms substituted in TiO_2 lattice helps in the process of photocatalytic reactions and why or

whether they are synergistic or antagonistic in nature? In our earlier communication [12], we have definitely established that if MoO_3 is present in the surface phase only it augments the photocatalytic oxidation more than that of TiO_2 anatase. However if it is present as a major bulk phase it is quite detrimental since in this case if we extrapolate the zeta potential values, MoO_3 should have further negative surface charge making the MB more stable on the surface. If an intermediate is very stable, then downhill reaction of its photo-oxidation will require more energy and will also follow a slower kinetics. .

From the results of EXAFS measurements on the samples as shown in Table-1 and Fig.8, we have indeed seen that there is a decreasing percentage of Mo as doped form and MoO_3 heterophase is incremented with increase in total concentration of Mo in the TiO_2 lattice and presence of MoO_3 in bulk form is maximum for the Mo-10 sample. This results in poorer photocatalytic performance of the Mo-10 sample compared to others. Thus it can be concluded that the performance of such a tri-phasic photocatalyst is controlled by the relative concentration of substitutional Mo ions to MoO_3 ratio, where the proper ratio of MoO_3 to that of Mo in substitutional sites makes it a good photocatalyst. However if there is a very high presence of bulk MoO_3 percentage and too low amount of Mo as substitutional dopant, it is detrimental for the photocatalytic effect. The MoO_3 and TiO_2 will form a heterojunction with an overall modification of their Fermi edges. The Mo-3d dopant will from a mid band gap step between the Ti -3d unoccupied conduction band and the O-1s occupied valence band [30]. Mo being in higher oxidation state may be used as an electron quencher thereby augmenting the lifetime of the holes. However going statistically the proper ratio of MoO_3 to that of substituted Mo makes it a good photocatalyst.

Results of photo-oxidation of MB over Mo incorporated titania samples under visible irradiation are included in Fig.9. The $t_{1/2}$ values as derived from Fig. 9 for Mo-1, Mo-2, Mo-5, Mo-10 and titania samples were found to be ~3.7, 3.5, 2.95, 16.1, 52.7 min, respectively, representing following trend in photocatalytic acivity for MB dye degradation: Mo-5 > Mo-2 > Mo-1 > Mo-10> TiO_2. The trend is same as that of the UV–irradiation with exception of that Mo-10, which is photocatalytically more active than TiO_2 with the visible irradiation. This is perhaps due to the fact that TiO_2 having a band gap of 3.24 eV is primarily a UV absorber while the Mo-10 sample posses a band gap of 2.65 eV [12] and is an absorber of visible radiation exhibiting better photocatalytic activity during degradation of MB.

4. Conclusion

From the EXAFS measurements on the Mo doped TiO_2 samples, it has been found that the experimental radial distribution function around Mo sites show signature of presence of both MoO_3 phase and substitutional Mo in TiO_2 lattice. It has further been observed by fitting of the FT-EXAFS spectra of the samples that as Mo doping concentration in TiO_2 increases, the percentage of Mo cation going into the TiO_2 lattice decreases and for 10% Mo doped sample about 93% of the Mo cations exist in MoO_3 phase and only 7% goes into the TiO_2 lattice. FT-IR spectra of the samples also show that there is a presence of the MoO_3 phase along with that of anatase TiO_2. From the photocatalytic data it is quite evident that there is a substantial amount of adsorption of the dye, thereby showing a good amount of electronic interaction of the dye with the catalytic surface. It has been further observed that the photocatalytic activity is higher for samples where MoO_3 phase is less and where Mo ions mostly resides in the substitutional sites in TiO_2 matrix. We can therefore conclude that the structural parameters will definitely play a

direct role in the photocatalytic degradation of the MB –dye by the Mo-TiO_2 catalysts, though, band gap may also play a role particularly in case of irradiation by visible light.

5. ACKNOWLEDGEMENTS

The authors wish to acknowledge the help of Dr. S. Pascarelli and Dr. O. Mathon in measuring the EXAFS data at ESRF. The authors also wish to acknowledge Dr. S. R. Bharadwaj, Chemistry Divivsion, BARC for discussion and support.

References

[1] A. Kubacka, M. Garcia, F. G. Colónb, *Chem. Rev.* 2012, **112**, 1555–1614

[2] B. O'Regan, M. Gr¨atzel, A Low-cost, Flms *Nature***,** 1991, **353**,737–740.

[3] M. Kitano, M. Matsuoka, M. Ueshima, M. Anpo, *Appl. Catal A: Gen.,* 2007, **325***,* 1–14.

[4] M. R. Hoffmann, S. T. Martin, W. Choi, D. W. Bahnemann, *Chem. Rev.*1995, *95*, 69–96.

[5] G. Devi, B. Murthy, L. Narasimha, *Catal. Lett.* 2008, *125,* 320-330.

[6] A. Fujishima, T. N. Rao, D. A. Tryk,, *J. Photochem. Photobio. C: Photochem Rev*. 2000 , **1**, 1–21.

[7] L. Sang, Y. Zhao, C. Burda, *Chem. Rev.*, 2014, **114,** 9283–9318.

[8] E. W. McFarland, H. Metiu, *Chem. Rev*. 2013, **113**, 391−4427.

[9] A. Kubacka, M. Fernandez Garcia, G. Colónb, *J. Cat.* 2008, **254,** 272–284.

[10] W. Li, A. I. Frenkel, J. C. Woicik, C. Ni, I. S. Shah, *Phys. Rev. B,*2005, **72** , 155315 (1-6).

[11] L. G. Devi, B. N. Murthy, S. G. Kumar. *Chemosphere* 2009**, 76**, 1163–1166.

[12] K. Bhattacharyya, J. Majeed, K. K. Dey, P. Ayyub, A. K. Tyagi, S. R. Bharadwaj, *J. Phys. Chem*. C, 2014, **118**, 15946-15962.

[13] Y J. Feng, C. Wang, W. R. Cheng, J. H. Huang, T. X. Zhao,.; Q. H. Liu,; Z. Xie, Z. Y. Pan, S. Q. Wei, *J. Phys*.: *Conference Series,* 2013, **430**, 012090.

[14] K. Schneider, M. Sikora, K. Cabbage, T. G. Michałów, A. Vital, M. Radecka, M. Rękas, D. Zajac, *Radiation in Natural Science,,* 2007**, 6**, 71.

[15] A. Kubacka, G. Colo´nb, M. Ferna´ndez-Garcı´a, *Cat. Today*, 2009, **143**, 286.

[16] http://www.rrcat.gov.in

[17] *X-Ray Absorption: Principles, Applications, Techniques of EXAFS, SEXAFS and XANES,* edited by D.C. Konigsberger and R. Prince (Wiley, New York, 1988).

[18] M. Newville, B. Ravel, D. Haskel, J. J. Rehr, E A. Stern, Y. Yacoby, *Physica B* 1995, **208,** 154-156.

[19] http://cars9.uchicago.edu/atomsdb/TiO_2-ana.inp.

[20] http://chemistry.osu.edu/~woodward/ch754/struct/MoO_3.html.

[21] S. Basu, D. Inamdar, S. Mahamuni, A. Chakrabarti, C. Kamal, G. Kumar, S. N. Jha, D. Bhattachharya, *J. Phys. Chem. C* 2014, **118***,* 9154–9164.

[22] L. Seguin‘, M. Figlarz‘.I, R. Cavagnat, J.C. Lasskgues, *Spectrochimiccra Acta:Part A* 1995, **51***,* 1323-1344.

[23] K. SrinivasaRao, B. RajiniKanth, P. K. Mukhopadhyay, *Appl. Phys A* 2009, **96**, 985–990.

[24] A. Klinbumrung, T. Thongtem, S. Thongtem, Synthesis of h- and α-MoO_3 *J. Nanomaterials* 2012, **930763**, 18-22.

[25] T. Ohsaka, F. Izumi, Y. Fujiki, *J. Raman Spectr.* 1978, **7,** 321-324.

[26] Y. H. Zhang, C. K. Chan, J. F. Porter, W. Guo, *J. Mater. Res*., 1998, **13,** 2602-2609.

[27] W. Choi, A. Termin, M. R. Hoffmann, *J. Phys. Chem* , 1994, **98**, 13669-13679.

[28] L. Xiong, W. Sun, Y. Yang, C. Chen, J. Ni, *J. Colloid and Interface Sc.* 2011, **356**, 211–216.

[29] R. E. Dawson, A. Hennig, D. P. Weimann, D. Emery, V. Ravikumar, J. Montenegro, T. Takeuchi, S. Gabutti, M. Mayor, J. Mareda, *et al. Nature Chemistry* 2010**, 2**, 533–538.

[30] C. Qiang, C. Hong-Hong, *Chin. Phys.* (Beijing, China) 2004, **13**, 2121−2125.

Figure Captions

1. $k^2\chi\ (k)$ verses k plot for different doping concentration of Mo in TiO_2 at Mo K edge.
2. Theoretical Radial Distribution ($\chi(r)$ versus r) plots around Mo sites for MoO_3 structure and Mo doped TiO_2 structure.
3. Experimental Radial Distribution ($\chi(r)$ versus r) plots for Mo doped TiO_2 samples around Mo sites along with best -fit theoretical plots assuming mixed phase of MoO_3 structure and Mo doped TiO_2 structure.
4. Experimental Radial Distribution ($\chi(r)$ versus r) plots for Mo doped TiO_2 samples around Ti sites along with best fit theoretical plots assuming TiO_2 structure.
5. **(A)**The IR spectra of the Mo-TiO_2 and TiO_2 materials (a) TiO_2–Anatase-nano (b) Mo-1 (c) Mo-2 (d) Mo-5 (e) Mo-10 (f) Mo-100. **(B)** shows detailed view between (1500 -400) cm^{-1} for Mo –TiO_2 samples.
6. Transmission electron microscopy pattern for the Mo-2 on the scale of (a) 5 nm, (b) 10 nm and (c) SAED pattern for the Mo-2 sample.
7. Plot of the time dependent photo-degradation of MB using all the photo-catalysts under UV-irradiation. This is a temporal plot of percentage of MB dye that is left after the photo-degradation by the individual photo-catalyst.
8. A) Plot of Mo-content in the TiO_2 and the $t_{1/2}$ value (representing the Left Y-axis); B) Plot of Mo doped percentile (percentage taking the Mo content to ne 100 %) in anatase lattice and the Mo-content in the TiO_2 (representing the Right Y-axis).
9. Temporal plot of the photo-degradation of MB using all the photo-catalysts under visible-irradiation.

Table Captions

1. Results of EXAFS Fitting of Mo doped TiO_2 at Mo K edge.

2. Results of TiO_2 structure fitting at Ti K edge

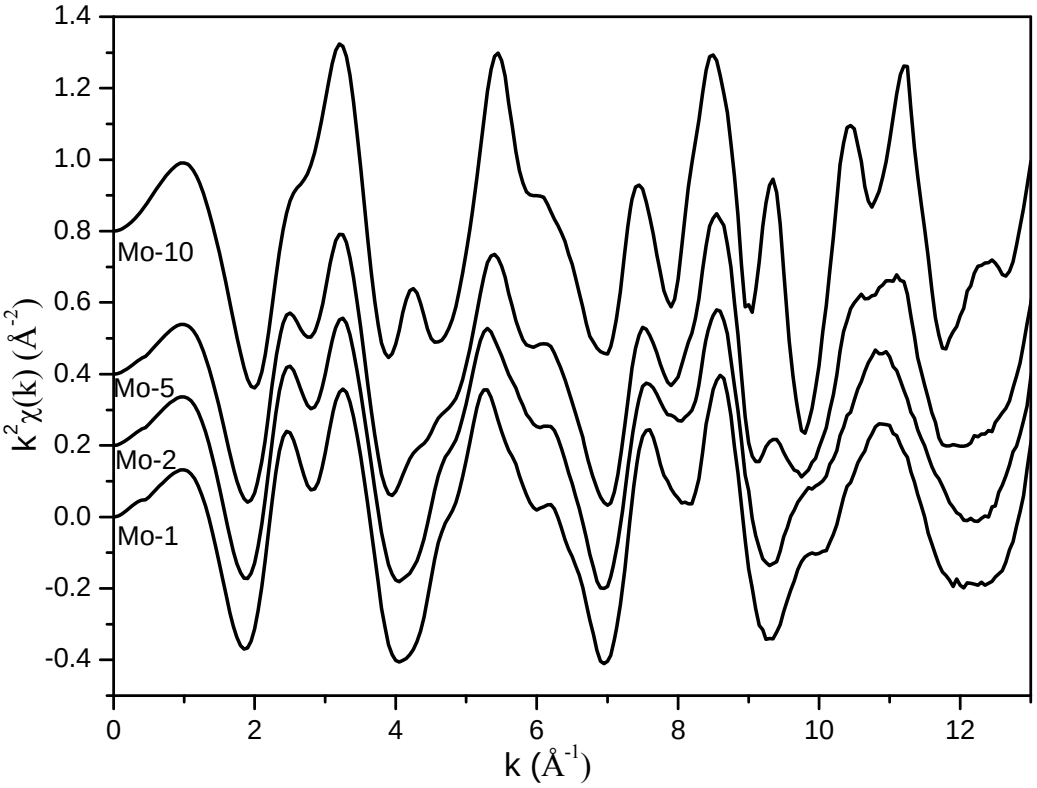

Figure -1

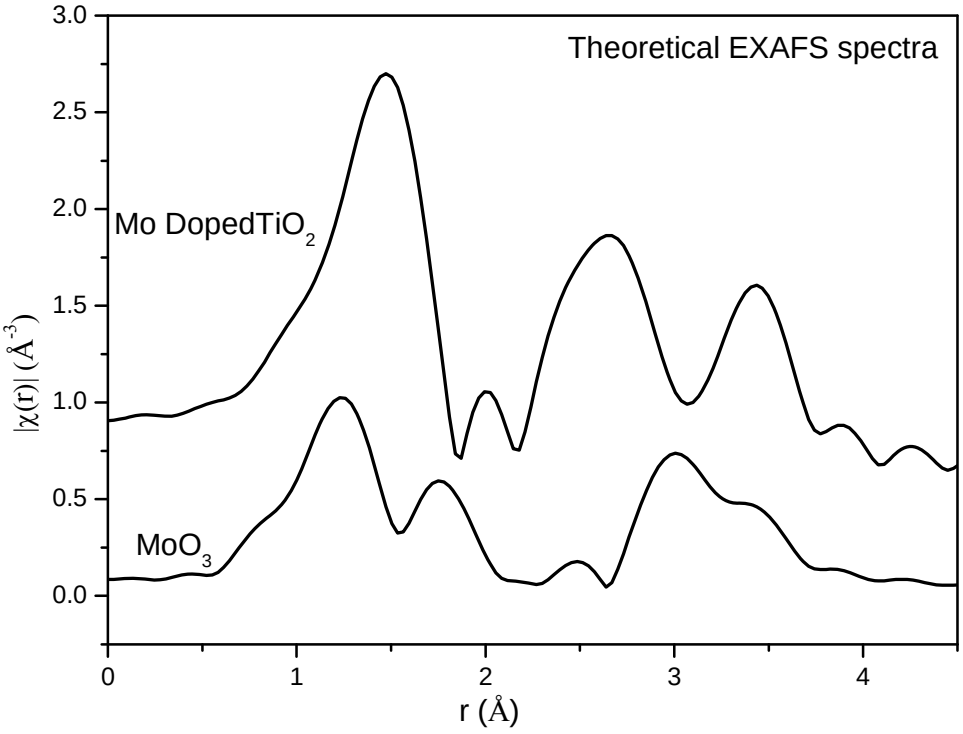

Figure 2

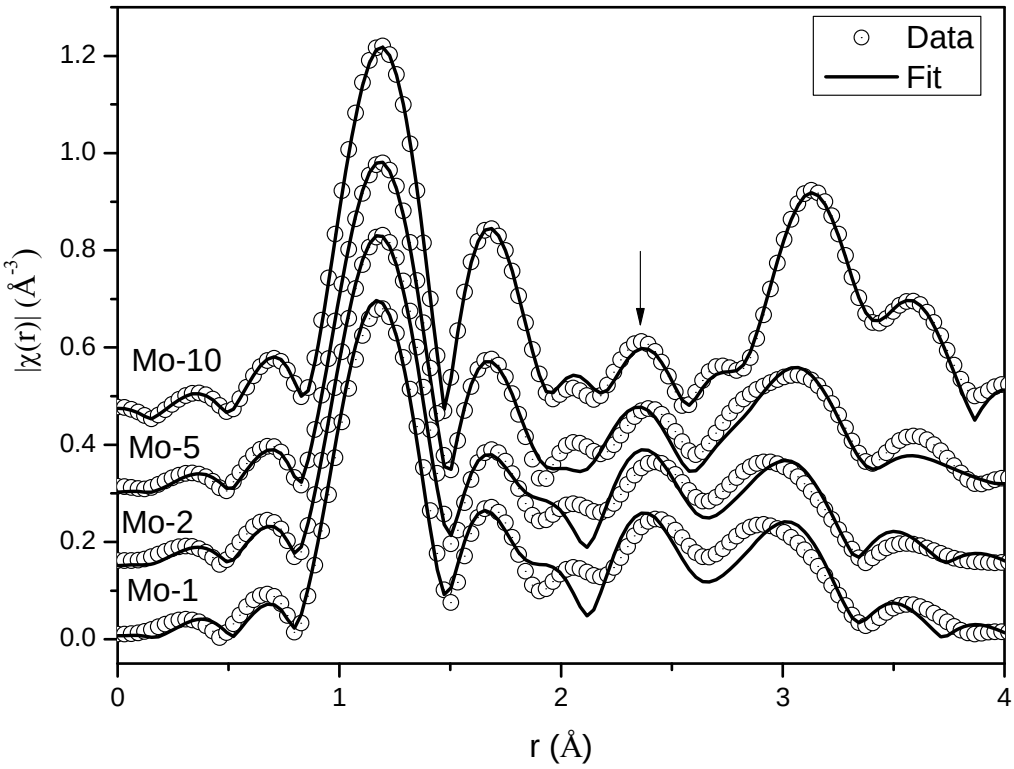

Figure 3

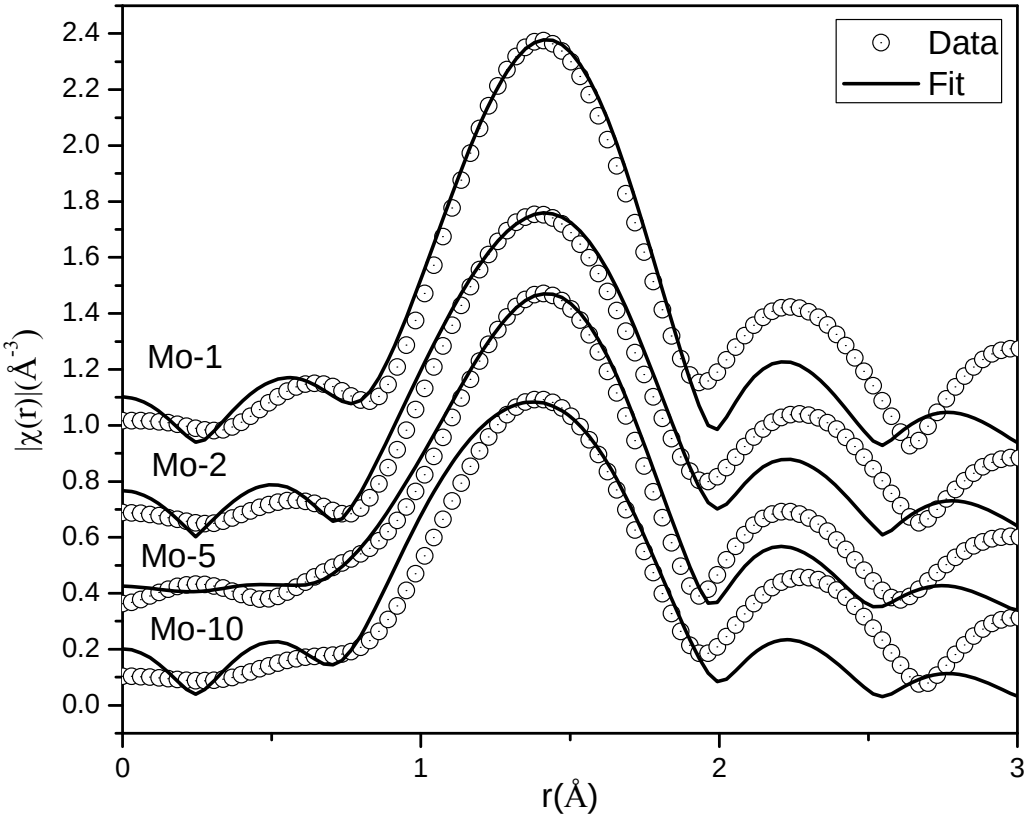

Figure- 4

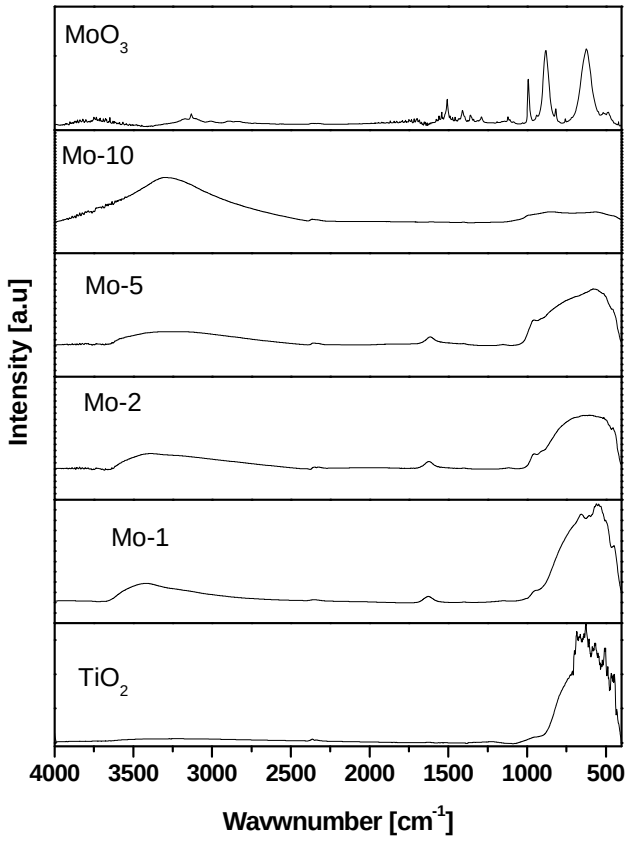

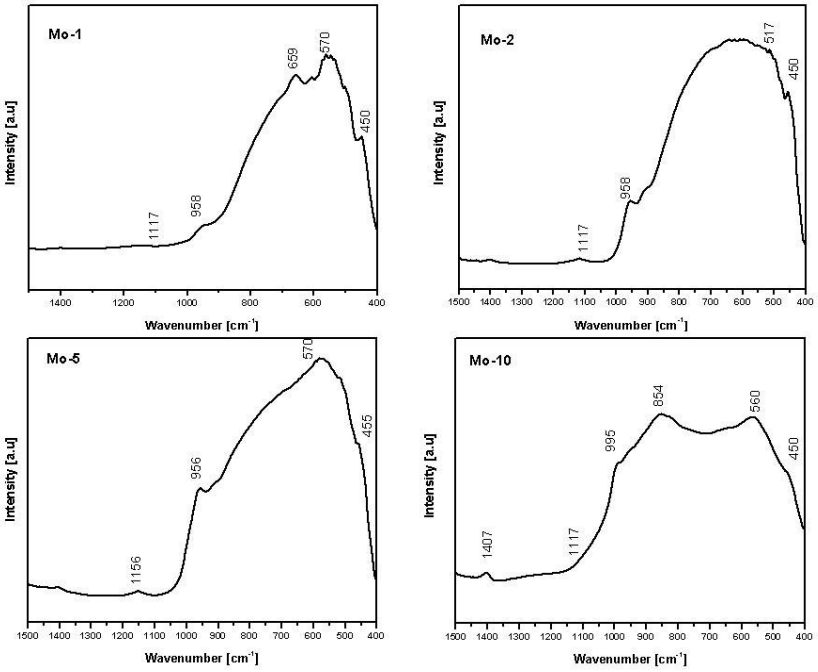

Figure- 5

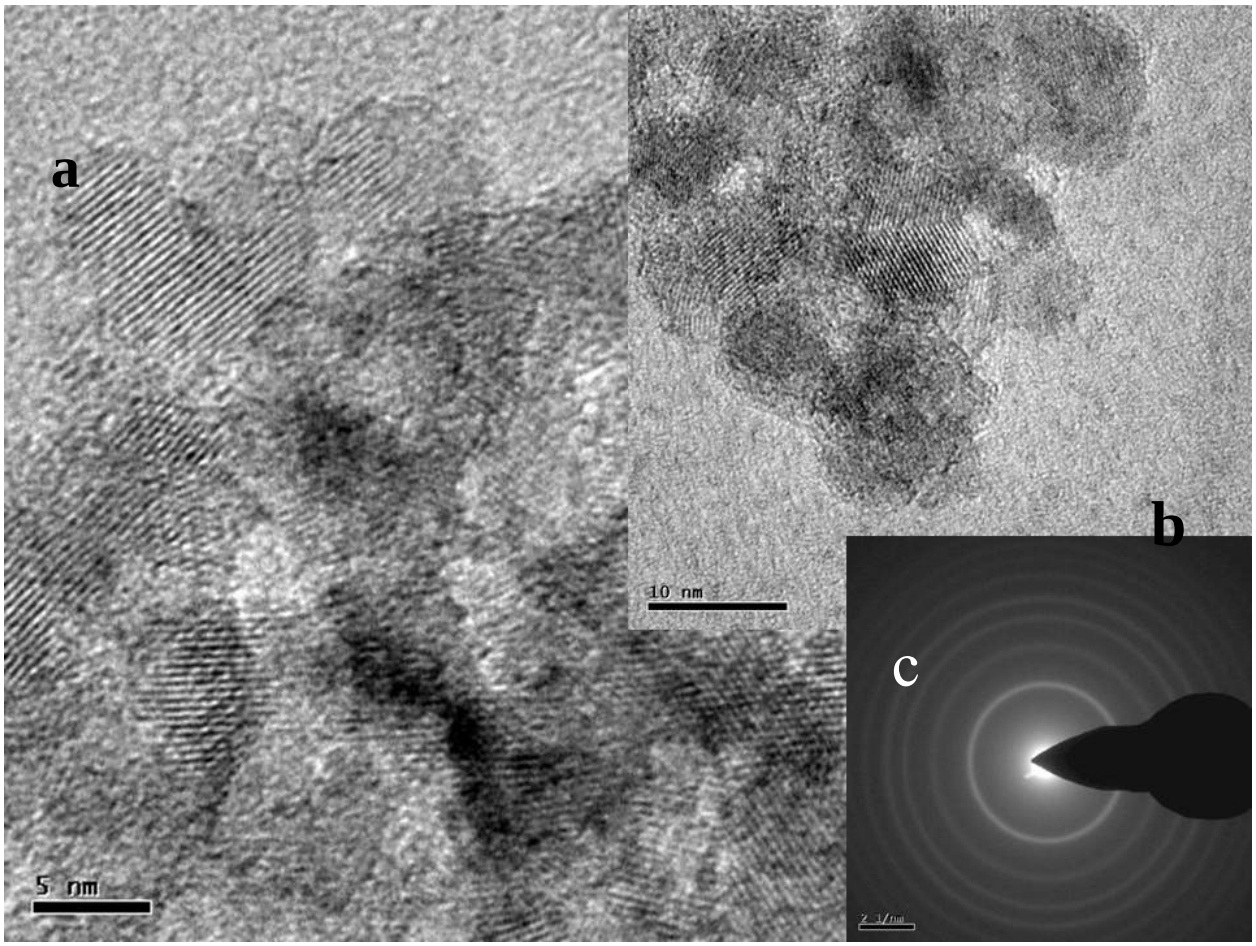

Figure- 6

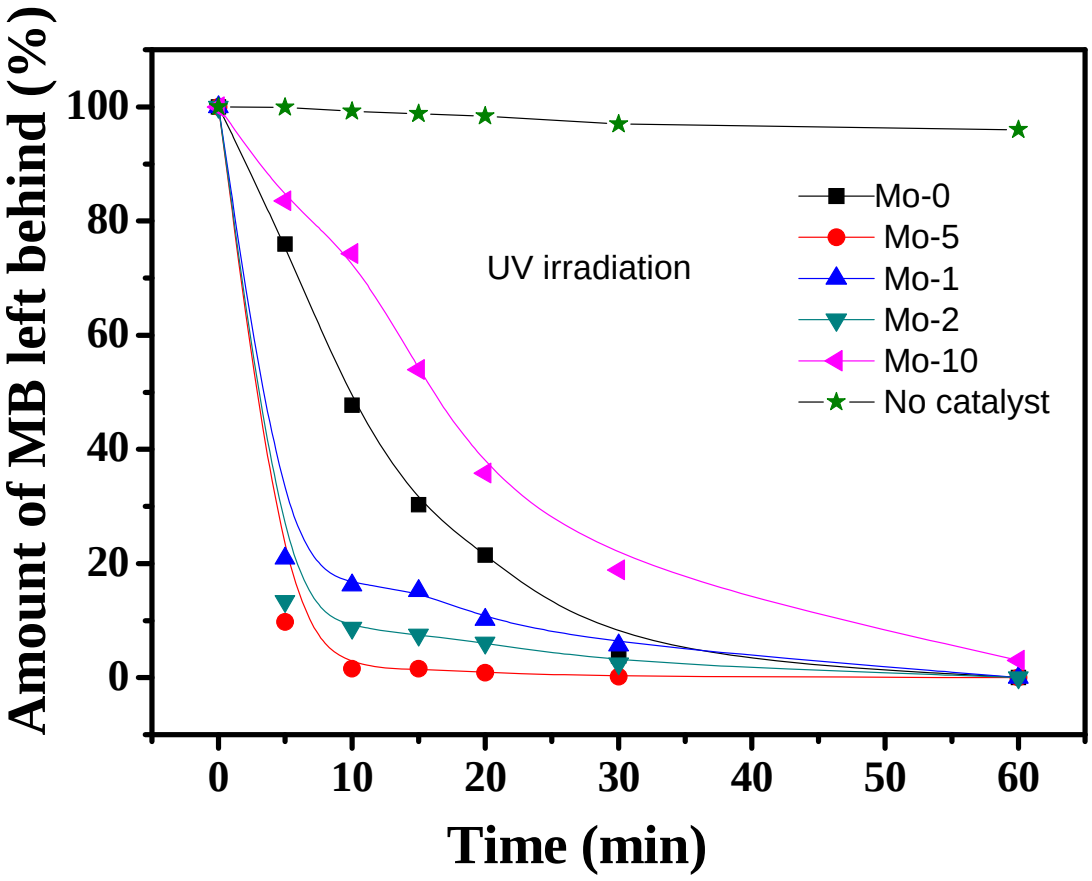

Figure- 7

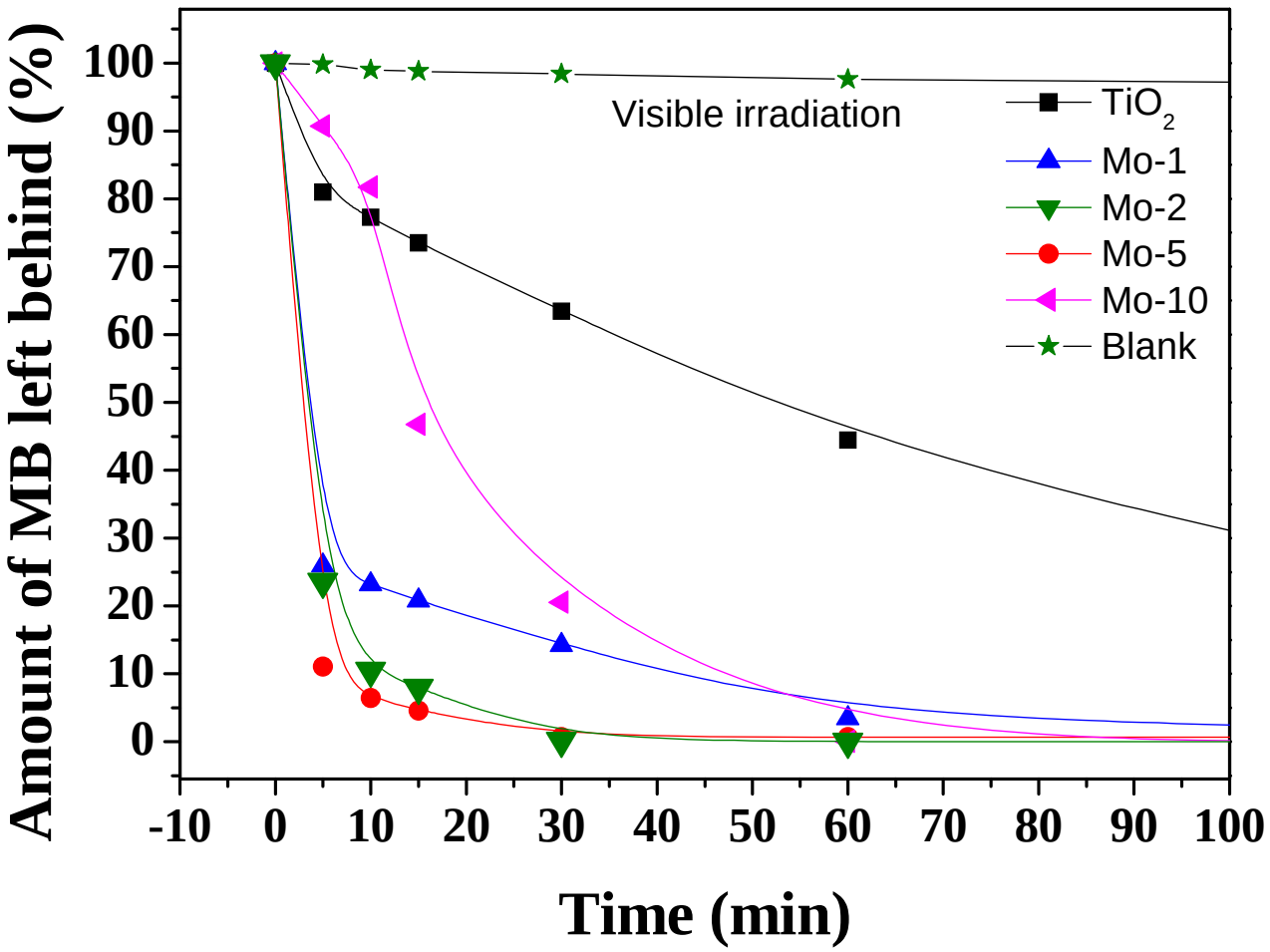

Figure- 9

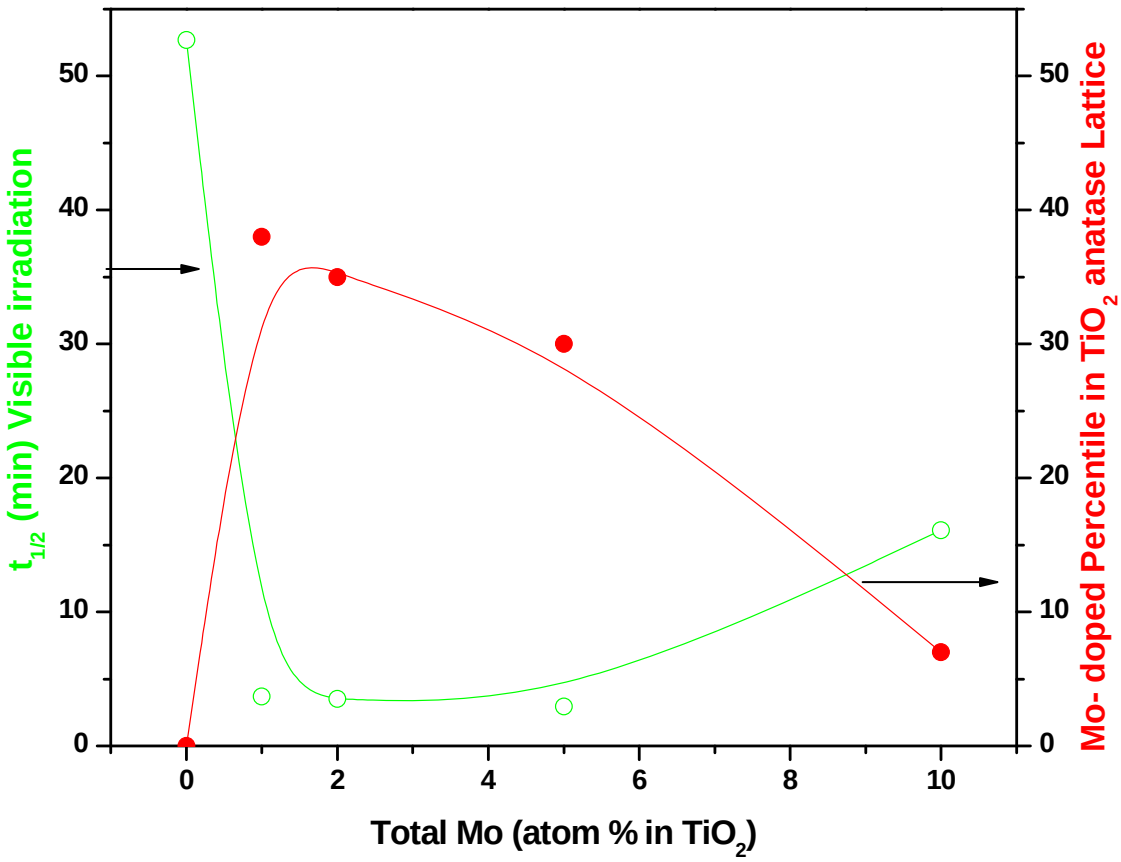

Figure- 8

Table 1:

	Mo-1		Mo-2		Mo-5		Mo-10	
MoO_3 Phase (x*100)	62(3)%		65(3)%		70(2) %		93(2)%	
	r (Å)	σ^2	r (Å)	σ^2	r (Å)	σ^2	r (Å)	σ^2
Mo-O1 (×2)	1.72(1)	0.003(1)	1.73(1)	0.003(1)	1.72(1)	0.003(1)	1.72(1)	0.003(1)
Mo-O2 (×2)	2.04(2)	0.016(2)	2.05(2)	0.012(4)	2.01(1)	0.007(1)	1.97(1)	0.005(1)
Mo-O3 (×2)	2.37(2)	0.008(3)	2.36(3)	0.009(1)	2.30(2)	0.009(2)	2.26(1)	0.007(1)
Mo-Mo1 (×2)	3.38(2)	0.007(3)	3.39(3)	0.008(3)	3.46(2)	0.013(2)	3.49(1)	0.007(1)
Mo-O4 (×4)	3.53(3)	0.012(3)	3.55(3)	0.014(3)	3.54(1)	0.006(1)	3.57(1)	0.009(2)
Mo-Mo2 (×2)	3.64(3)	0.016(6)	3.65(3)	0.015(4)	3.78(2)	0.012(3)	3.79(1)	0.006(1)
Mo in TiO_2 Phase ((1-x)*100)	38(3)%		35(3)%		30(2)%		7(2)%	
	r (Å)	σ^2	r (Å)	σ^2	r (Å)	σ^2	r (Å)	σ^2
Mo-O (×6)	1.86(1)	0.023(3)	1.87(1)	0.022(1)	1.87(1)	0.021(2)	1.82(1)	0.02(2)
Mo-Ti/Mo (×4)	2.90(2)	0.010(3)	2.91(2)	0.010(2)	2.92(1)	0.011(1)	2.95(2)	0.006(3)

Table 2

	Theoretical		Mo-1		Mo-2		Mo-5		Mo-10	
	r(Å)	N	r(Å)	σ^2	r(Å)	σ^2	r(Å)	σ^2	r(Å)	σ^2
Ti-O(×6)	1.94	6	1.95(2)	0.007(2)	1.94(1)	0.010(3)	1.93(2)	0.012(2)	1.93(2)	0.013 (2)

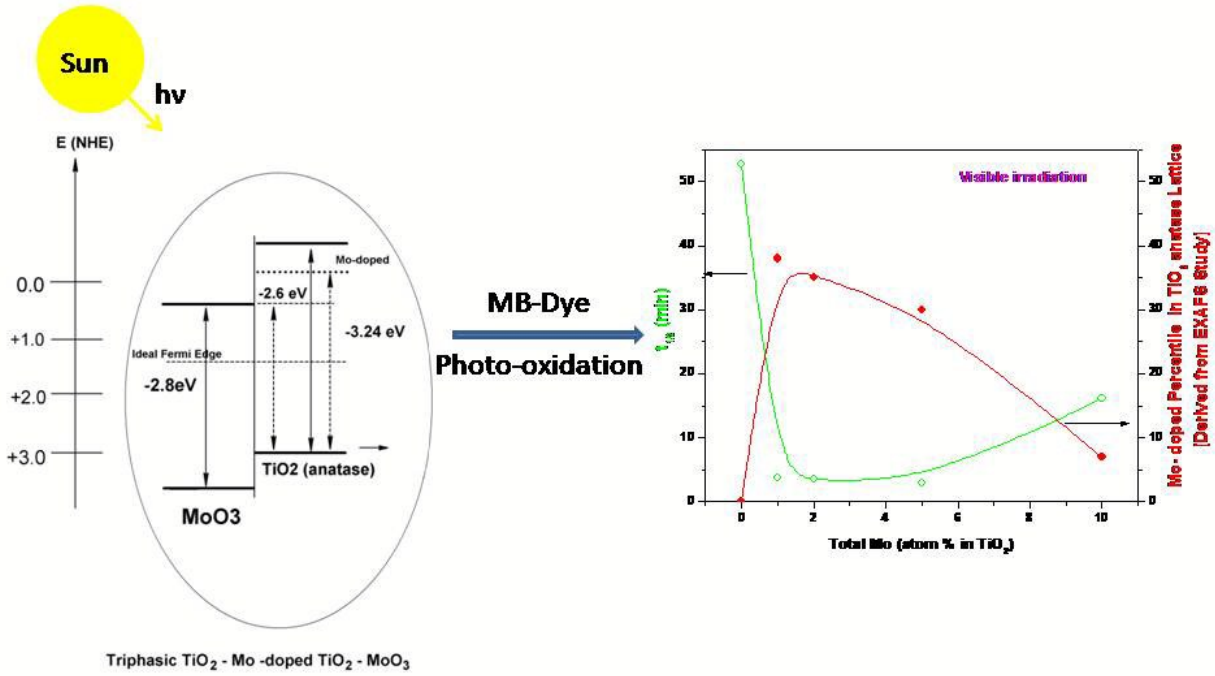

Triphasic TiO_2 - Mo -doped TiO_2 - MoO_3

TOC